KfK 3198
Oktober 1981

Internal Cluster Beam Target for Antineutron Production in LEAR

J. Gspann, H. Poth
Institut für Kernphysik
Institut für Kernverfahrenstechnik

Kernforschungszentrum Karlsruhe

KERNFORSCHUNGSZENTRUM KARLSRUHE

Institut für Kernphysik
Institut für Kernverfahrenstechnik

KfK 3198

Internal Cluster Beam Target for Antineutron Production in LEAR

J. Gspann and H. Poth

Kernforschungszentrum Karlsruhe GmbH, Karlsruhe

Kernforschungszentrum Karlsruhe GmbH
ISSN 0303-4003

INTERNAL CLUSTER BEAM TARGET FOR ANTINEUTRON PRODUCTION IN LEAR

J. Gspann and H. Poth

Kernforschungszentrum Karlsruhe
Institut für Kernverfahrenstechnik

and

Institut für Kernphysik
Postfach 3640, 7500 Karlsruhe, Federal Republic of Germany

Abstract

An internal hydrogen cluster beam target dedicated to antineutron production is proposed for installation in one of the bending magnets of LEAR. Running in the wedge-shaped gap in the center of the magnet, the cluster beam will intersect the antiproton beam vertically. The design target thickness is 2×10^{-10} g/cm^2, with lower values being readily available. The antineutron production rate is expected to be larger than 5.5×10^4 $\bar{n}$/s at 600 MeV/c and optimum target thickness. The cluster beam source will be located on top of the magnet together with its main pumping stages while the main sink stages will be placed below the magnet. Turbomolecular pumps will be used for pumping the higher gas loads at the source as well as for removing the main part of the beam flux. For the intermediate pumping stages, refrigerator cryopumps are proposed. Later installation of the facility in a long straight section of LEAR would be possible.

Part of proposal to the CERN PSCC; CERN/PSCC/81-27, PSCC/P41, March 1981

Ein internes Clusterstrahltarget zur Antineutronproduktion im LEAR

J. Gspann und H. Poth

Kernforschungszentrum Karlsruhe GmbH
Institut für Kernverfahrenstechnik
und
Institut für Kernphysik

Zusammenfassung

Es wird ein internes Wasserstoff-Clusterstrahltarget zur Installation in einem der Ablenkmagnete von LEAR für Antineutronproduktion vorgeschlagen. Nach der Passage des keilförmigen Spaltes im zentralen Magnetblock kreuzt der Clusterstrahl den Antiprotonenstrahl in vertikaler Richtung. Als Targetdicke ist $2 \cdot 10^{-10}$ g/cm^2 vorgesehen. Niedrigere Werte können ebenso eingestellt werden. Eine Antineutronrate von mehr als $5{,}5 \cdot 10^4$ pro sec bei 600 MeV/c Antiprotonenimpuls und optimiertem Betrieb wird erwartet. Die Clusterstrahlquelle mit ihren Hauptpumpstufen wird über dem Magneten installiert, während der Strahlsumpf unter dem Magneten aufgebaut wird. Der höhere Gasanfall in Quellen- und Sumpfnähe wird mit Turbomolekularpumpen abgepumpt. Für die dazwischen liegenden Stufen sind Kryopumpen vorgesehen. Ein Einbau dieses Clusterstrahltargets in eine lange gerade Sektion von LEAR wäre auch möglich.

INTERNAL CLUSTER BEAM TARGET FOR ANTINEUTRON PRODUCTION IN LEAR

J. Gspann and H. Poth

Kernforschungszentrum Karlsruhe
Institut für Kernverfahrenstechnik

and

Institut für Kernphysik
Postfach 3640, 7500 Karlsruhe, Federal Republic of Germany

INTRODUCTION

The use of an internal target for the in-flight study of $N\bar{N}$ interactions has been a central point in the discussions[1-6] of the physics possibilities at LEAR[7], especially when considering the future program.[8-12] In particular, it turned out that such a target is of great value for the production of antineutrons,[5,6] which are a unique strong interaction probe for investigating $N\bar{N}$ interactions.[13,14] On an internal hydrogen target, the antineutrons can be produced with high momentum resolution and efficiency, primarily in the forward direction, through the antiproton charge exchange reaction.

The operation of an internal target requires a strong beam cooling to compensate the beam blow up, in particular at low energies. This can be achieved in LEAR earlier than foreseen by making use of the ICE electron cooling equipment.[15] (At higher energies stochastic cooling will suffice).

Target densities adequate for full exploitation of this facility can be obtained with a hydrogen cluster beam as an internal target.

Cluster beams, or condensed molecular beams, of hydrogen as well as other gases have been studied and developed for quite a period of time at the Kernforschungszentrum Karlsruhe, aiming mainly at fuel injection into fusion

machines.[16-18] Based on the results of these investigations, internal cluster beam targets have been build, or are under construction, for SATURNE, Saclay,[19] as well as for SPS[20] and ISR.[21]

Cluster beams are distinguished by their high intensity and the high directivity of their mass flow. Hence, they show sharply bounded intensity profiles, providing a well defined beam interaction region, and the least possible gas load on the ring vacuum.

We propose the development and construction of a hydrogen cluster target to be installed in the wedge-shaped central gap of one of the bending magnets of LEAR. This location would give full access to the antineutrons produced in the forward direction, dominating at low momenta, as they leave the ring unaffected by the magnetic field.

CLUSTER BEAM

Figure 1 shows a vertical cross section of the planned set-up schematically, with somewhat more detail for the part inside the wedge-shaped magnet gap. The cluster beam is formed by expansion of precooled gas through a converging-diverging cold nozzle and passes the source pressure stages 1 to 4 as well as the LEAR vacuum casing 5 to reach the sink stages 6 to 8. A short summary of the preliminary specifications is given in Table 1.

Geometry

The geometry of the cluster beam is determined by the required width at the intersection with the antiproton beam as well as the magnet dimensions. For the antiproton beam, a horizontal width at the center of the magnet of at most 30 mm is expected to be achievable by electron cooling (see Appendix). Allowing for an orbit deviation of $\pm$ 5 mm, the target width is chosen to be 40 mm. For economic use of the flow through the axial symmetric nozzle, the target depth is, presently, also chosen to be 40 mm. In order to illuminate this rather large cross sectional area, proven technology of cluster beam generation requires large distances to the source nozzle since the condensed part of the nozzle flow is typically confined within about $\pm 2^{\circ}$ of angular divergence.[17]

Low divergence of the cluster beam is also advantageous with respect to the size of the apertures between the sink pressure stages which should be kept as small as possible. A distance of 1 m between the intersection of the beam axes and the throat of the nozzle is proposed. This distance will allow to place the main source pumping stages on top of the magnet, providing sufficiently large suction cross sections near the collimating orifices. Similarly, the main sink pumps have to be installed below the magnet.

Source

The source nozzle will have a throat diameter of 0.15 mm, a full apex angle of 10^{o}, and a length of 25 mm of the diverging part. The nozzle will be cooled to 20-30 K by a closed cycle refrigerator. The first orifice in the nozzle flow, called skimmer, will be cooled to about nozzle temperature, while the following collimators will be kept at about 80 K and room temperature, respectively.

Target thickness

With a cluster beam intensity of 10^{22} H_2 molecules per steradian and second, which is expected to be safely achievable in continuous beam operation, a target thickness of 2×10^{-10} g H_2/cm^2 will be obtained. (The higher intensity values reported in recent years have always been obtained in pulsed beam operation). Lower values of the target thickness can be reached by lowering the gas flow through the nozzle, as well as by using nozzles of smaller throat diameters.

Sink

The beam dump or sink is presently considered as the part demanding the largest development efforts. This is mainly due to the required large beam cross section which implies even larger apertures between the following sink stages. At present, we envisage a turbomolecular pump as the final stage. A grid of highly polished cluster reflectors at optimum temperatures, i. e. about 220 K for hydrogen clusters,[22] will be used to deflect the clusters

by about 10^{o} so that they may pass the slots of the first disk with the least possible disturbance. (Presumably, the tilt angle of the teeth of the first disk will have to be adjusted, too). The array of cluster reflectors will also serve to reduce the conductance between the pressure stages 8 and 7. Tubular extensions from the apertures between stages 5 and 6, as well as 6 and 7, will serve the same purpose.

Pumps

Turbomolecular pumps of a total nominal speed of 2×10^{4} 1/s are envisaged for the first two pumping stages. The actual pumping speed at the pressure of the first stage, 10^{-2} mbar, is expected to be 5000 1/s. About this pumping speed is required also for the second pressure stage as well as for the sink turbopumps. A three stage backing pump system of two Roots stages with 4000 m^3/h and 500 m^3/h pumping speed and a forepump stage of 120 m^3/h pumping speed are planned.

For the intermediate pressure stages 3, 4, 6, and 7, refrigerator cooled cryosorption pumps are proposed. The largest of these with 2.5×10^{4} 1/s pumping speed is planned for the sink stage 7. Table 2 summarizes the respective apertures, conductances, and pumping speeds, as well as the expected stage pressures and gas fluxes.

Valves

In order to separate the LEAR vacuum system from the source and sink stages of the internal target, valves are planned to be located within the wedge-shaped gap. They are necessary, in particular, when the cryosorption pumps will be regenerated, providing then appreciable amounts of gas. These valves could be chosen to be all metal bakeable valves. Valves are also planned to separate the turbomolecular pumps from the source stages 1 and 2 in order to allow a separate venting of these pumps.

Backflow

As shown by Tab. 2, the flow into the LEAR vacuum will be determined by the backflow from the beam dump. It is expected to be of the order of 2×10^{-4} times the beam flux B. This value being considered as an optimistic rather than a conservative estimate, a value of about 5×10^{-4} B is quoted in Tab. 1. If an effective pumping speed of 2000 l/s is assumed at LEAR, a pressure bump of 1.6×10^{-7} mbar would result in LEAR from 5×10^{-4} B inflow. If this pressure bump could be confined to a length of 300 cm along the ring, it would correspond to a target thickness of $4{,}3 \times 10^{-12}$ g H_2/cm^2, that is about 2 % of the design target thickness.

It should be noted that a reduction of the design target depth from 40 to 10 mm, at the expense of beam generation economy, leading to a corresponding reduction of the conductances between the pressure stages 5 to 7, but assuming unchanged flow from 8 to 7, would result in a reduction of the estimated backflow into LEAR by an order of magnitude.

Operation

The lay-out of the facility presented here should allow an uninterrupted operation for several months as far as the capacity of the refrigerator cryopumps is concerned. Heavier beam gases, except helium, could be used without major changes.

The beam flow could be stopped during the refilling of LEAR by closing the inlet valve for the source gas. By changing the inlet pressure, the target thickness could be changed within minutes. It would be determined by measuring the cluster beam intensity with a stagnation pressure probe. The cluster beam could be intercepted for signal recovery purposes by a rotating disk beam chopper installed in the second or third pressure stage.

INSTALLATION IN LEAR

The cluster beam target could be installed in the bending magnets BH1 or BH2 of LEAR (Fig. 2) according to the available space for experimental equipment and the final lay-out of the area. We have discussed here only the installation of the system in one of the bending magnets of LEAR for antineutron production. The outlined concept of the cluster beam target is however also suitable for the installation in a straight section of LEAR if the necessary space for the pumping system is provided and modified according to the experimental apparatus. Then an even larger variety of experiments can be performed. Details of the LEAR operation with an internal target for antineutron production are given in Ref.[23].

ANTINEUTRON PRODUCTION RATES AND BEAM PROPERTIES

The kinematics of the charge exchange reaction and the internal target operation for antineutron production are outlined in the Appendix. The expected integral antineutron production rates for optimal operation conditions are shown in Fig. 4. The number of antineutrons produced into a forward solid angle of 1.7 mstrd (acceptance of the tangential vacuum extension tube) and into a solid angle of 14 mstrd (possible external target at closest distance to the magnet) are shown in Fig. 7. The required cooling times to achieve a given equilibrium beam emittance are shown in Fig. 8.

REFERENCES

1. U. Gastaldi, K. Kilian and G. Plass, A Low-energy antiproton facility at CERN: Physics possibility and technical aspects, CERN:PSCC/79-17, 25 May 1979.

2. K. Kilian and D. Möhl, Gas jet target in LEAR, $\bar{p}$ -LEAR Note 44.

3. P. Dalpiaz and K. Kilian, Prolarization with LEAR, $\bar{p}$ -LEAR Note 31.

4. W. Kubischta, The CERN polarized atomic hydrogen target, $\bar{p}$-LEAR Note 17.

5. C. Voci, Antineutrons at LEAR, in Proceedings of the Workshop on Physics with Cooled Low Energetic Antiprotons, Karlsruhe, March 19-21, 1979 (ed. H. Poth) (KFK-Report 2836) and $\bar{p}$-LEAR Note 71 and Antineutron beam at LEAR, $\bar{p}$-LEAR Note 20.

6. H. Poth, Antiproton charge exchange and antineutron interactions, $\bar{p}$-LEAR Note 51.

7. Design study of a facility for experiments with low energy antiprotons (LEAR) (ed. G. Plass), CERN/PS/DL 80-7, 1980.

8. A.S. Clough et al, Letter of Intent for an experiment at LEAR, CERN/PSCC/79-66, PSCC/I 16.

9. E. Heer et al, Letter of Intent, CERN/PSCC/79-641, PSCC/I 14.

10. K. Kilian, Comment concerning internal gas targets in LEAR, Memorandum to the PSCC, CERN/PSCC/80-81, PSCC/M47.

11. J.C. Kluyver, Study of bargonium states with LEAR, Letter of Intent, CERN/PSCC/80-101, PSCC/I 21.

12. H. Poth, Study of the antiproton charge exchange reaction and antineutron interactions at low energies, Letter of Interest, CERN/PSCC/80-26, PSCC/I 24.

13. H. Haseroth, CH. Hill, P. Möller-Petersen and H. Poth, On the use of the ICE-gun for electron cooling in LEAR, CERN/PS/LR/Note 80-7.

14. H. Poth and J.-M. Richard, Low energy proton antiproton charge exchange and applications, contribution to IX Int. Conf. on High Energy Physics and Nuclear Structure, Versailles, July 1981.

15. K. Kilian, H. Poth and J.-M. Richard, Physics with an internal target for $\bar{n}$-production at LEAR, Memorandum to the CERN PSCC: CERN/PSCC/81-46, PSCC/M90, May 1981

16. E.W. Becker, K. Bier and W. Henkes, Strahlen aus kondensierten Atomen und Molekeln im Hochvakuum, Z. Physik 146, 333 (1956).

17. W. Obert, Properties of cluster beams formed with supersonic nozzles, Rarefied gas Dynamics, 11th Symposium, (R. Campargue ed.) CEA Paris 1979, p. 1181.

18. E.W. Becker, H.D. Falter, O.F. Hagena, W. Henkes, R. Klingelhöfer, H.O. Moser, Entwicklung eines Clusterionenbeschleunigers für die Fusionstechnik, KfK-Nachrichten 11(2), 3 (1979), and references cited therein.

19. M. Garçon (Private Communication)

20. CERN-Lausanne-Michigan-Rockefeller Collaboration, SPSC/80-63, SPSC/P 148 (1980).

21. Annecy (LAPP)-CERN-Frascati-Genova-Lyon (IPN)-Oslo-Roma-Torino Collaboration, Charmonium Spectroscopy at the ISR using an antiproton beam and a hydrogen jet target, ISRC/80-14, ISRC/P 106 (1980).

22. J. Gspann and G. Krieg, Reflection of clusters of helium, hydrogen, and nitrogen as function of the reflector temperature, J. Chem. Phys. 61, 4037 (1974).

23. M. Giesch, J. Gspann, K. Kilian, P. Lefèvre, D. Möhl, H. Poth and R. Riboni, Implications of an internal target for antineutron production in LEAR CERN/PS/DL LEAR Note 81-4 and $\bar{p}$ LEAR Note 93, 1981

Table 1

Summary of preliminary specifications

H_2 target thickness	2×10^{-10} g/cm^2
target depth x width	4 x 4 cm^2
distance from nozzle	100 cm
nozzle temperature	20 K
nozzle throat diameter	0.15 mm
nozzle throughput F	50 mbar l/s
pressure at 1st stage, p_1	10^{-2} mbar
total nominal pumping speed of source turbos	2×10^4 l/s
actual pumping speed at 1st stage at p_1	5×10^3 l/s
beam flux B	1.6×10^{19} molecules/s $\cong$ 0.013 F
expected dump backflow	6×10^{-6} F $\cong$ 5×10^{-4} B
estimated costs	930 kDM

Table 2

Pressure stage specifications

Pressure stage	S_{eff} 10^3 1/s	L 1/s	p mbar	J mbar 1/s
1	5	17.9	10^{-2}	50
2	5	26.5	3.6×10^{-5}	0.18
3	5	34.2	2×10^{-7}	9.5×10^{-4}
4	1	553	4.4×10^{-9}	6.8×10^{-6}
5	2		6.8×10^{-8}	1.37×10^{-4}
6	1	800	1.7×10^{-7}	3×10^{-4}
7	25	1000	3×10^{-7}	7.9×10^{-3}
8	33	400	2×10^{-5}	0.65

S_{eff} = effective pumping speed

L = conductance to next stage facing LEAR

p = stage pressure

J = mass flow into stage

APPENDIX

Kinematics of the reaction $\bar{p}p \to \bar{n}n$

The threshold for the charge exchange reaction corresponds to a CM-energy S_0 and antiproton momentum $p^0_{\bar{p}}$ of

$$\sqrt{s_0} = 1879 \text{ MeV} \qquad p^0_{\bar{p}} = 98 \text{ MeV/c}$$

Antineutrons originating from the charge exchange reaction are produced into a forward cone with a maximum opening angle of

$$\cos\theta_{max} = \frac{p^0_{\bar{p}}}{p_{\bar{p}}} \cdot \frac{s}{s_0} \approx 2.8 \cdot 10^{-5} \frac{s}{p_{\bar{p}}}$$

The antineutron momentum for the maximal production angle is

$$p_{\bar{n}}\,(\theta_{max}) = \frac{1}{2}\, p^0_p = 49 \text{ MeV/c}$$

The antineutron momentum spectrum extends from

$$p^{min}_{\bar{n}} = \frac{1}{2}\,(p_{\bar{p}} - \sqrt{p^2_{\bar{p}} - p^{0\,2}_{\bar{p}}}) \quad \text{to} \quad p^{max}_{\bar{n}} = \frac{1}{2}\,(p_{\bar{p}} + \sqrt{p^2_{\bar{p}} - p^{0\,2}_{\bar{p}}})$$

There exists a twofold ambiguity between the antineutron production angle and its momentum in the laboratory system

$$p_{\bar{n}} = \frac{1}{2}\left\{p_{\bar{p}}\,\frac{\cos\theta}{\alpha} \pm \sqrt{4\gamma^2\,\frac{m_n^2 + m_p^2}{\alpha} - p^2_{\bar{p}}\,\frac{\cos^2\theta}{\alpha^2}}\right\}$$

with $\gamma^2 = s/4m_p^2$, $\alpha = \gamma^2\sin^2\theta + \cos^2\theta$ which leads to a high energy ($p_{\bar{n}} > \frac{1}{2}\, p^0_{\bar{p}}$) and a low energy component ($p_{\bar{n}} < \frac{1}{2}\, p^0_{\bar{p}}$) in the antineutron spectrum (Fig. 3).

The low energy component corresponds to backward production in the CM-system so that

$$\sin\theta^* \leq \frac{p^0_{\bar{p}}}{p_{\bar{p}}}\,\frac{s}{s_0} \qquad \theta^* \text{ CM production angle} \qquad (1)$$

In the case of an isotropical production in the CM-system, the difference between the high energy and the low energy antineutron rate $\Delta N_{\bar{n}}$ is

$$\Delta N_{\bar{n}} = 2\cos\theta^{*}_{max} \cdot R_{\bar{n}} \qquad R_{\bar{n}} : \text{total antineutron rate}$$

where θ^{*}_{max} is defined by the equal sign in equation (1).

Due to these kinematics the antineutron rate observed in given forward solid angle is strongly enhanced in the laboratory system close to the threshold.

Internal target thickness

Densities of a few 10^{-10} g/cm^2 are expected to be safely achievable with continuous molecular cluster beams and to be acceptable for the ultra-high vacuum in LEAR. In the following we work out the optimal operation condition of such a target in LEAR.

A stored beam undergoes Coulomb or strong interactions when it traverses the target. Small angle scattering sums up with each passage and produces a beam blow-up which leads to unwanted beam losses. This multiple scattering blow-up can be compensated by a cooling system which achieves transverse cooling times smaller than the multiple scattering blow-up time. Then the beam losses are reduced to scatters larger than the machine acceptance or to inelastic reactions. In this case and in the absence of other losses (resonances, rest gas, beam extraction) the stored beam intensity decays as

$$\frac{N_{\bar{p}}}{N_{\bar{p},0}} = e^{-\sigma L \rho d f t}$$

$N_{\bar{p},0}$ = number of initially stored antiprotons

$f = \frac{\beta c}{u}$ = revolution frequency

u = machine circumference = 78.54 m

L = Avogadro's number

βc = velocity of the circulating antiprotons

with a time constant

$$\tau = \frac{1}{\sigma \cdot L \cdot \rho d \cdot f} \qquad \rho d = \text{target thickness in g/cm}^2$$

$$= \frac{u}{L \cdot \rho d \cdot \beta\sigma \cdot c} \qquad \sigma = \Delta\sigma + \sigma_{st} \qquad (2)$$

The total cross-section σ can be decomposed into a cross-section for Rutherford scattering under angles larger than the machine acceptance θ_0.

$$\Delta\sigma = \sigma_{Ruth}(\theta > \theta_0) = \frac{\pi r_p^2}{(\gamma - 1)^2 \theta_0^2} \qquad (3)$$

r_p = classical proton radius

$= 1.53 \quad 10^{-16}$ cm

$\gamma = (1 - \beta^2)^{-\frac{1}{2}}$

θ_0 in rad

and into the strong interaction cross-section σ_{st} which can be parametrized [1] as

$$\sigma_{st} = \frac{55.4}{p_{\bar{p}}} + 60.5 \text{ mb} \qquad p_{\bar{p}} \text{ in GeV/c} \qquad (4)$$

While $\beta\sigma_{st}$ varies only little with the antiproton momentum, the Coulomb scattering dominates at low momenta. Since the Rutherford scattering is inversely proportional to the square of the cut-off scattering angle, an increase of the machine acceptance angle θ_0 reduces the Coulomb losses at low energies considerably.

The optimal operation condition is achieved for a given $\bar{p}$ momentum if the target density and the number of initially stored antiprotons are adjusted in such a way that the antiproton interaction reaction rate equals the antiproton accumulation rate (assumed to be 10^6/sec.) The refilling cycle is then determined by the beam lifetime in LEAR given by (2).

With a fixed target density of $2 \cdot 10^{-10}$ g/cm^2 this condition is met, for instance, at 150 MeV/c with 10^9 initially stored antiprotons and at 2 GeV/c with $2.5 \cdot 10^{10}$ $\bar{p}$ for an acceptance angle of 6 mrad. The corresponding accumulation time is then 10^3 sec and $2.5 \cdot 10^4$ sec, respectively.

Antineutron rates

The number of antineutrons produced in the charge exchange reaction for a given target thickness ρd and a given number of stored antiprotons $N_{\bar{p}}$ is

$$R_{\bar{n}} = N_{\bar{p}} \cdot L \cdot \sigma_{CEX} \cdot \rho d \cdot f = N_{\bar{p}} \cdot L \cdot \beta\sigma_{CEX} \cdot \rho d \cdot \frac{c}{u} \qquad (5)$$

Combining (2) and (5) we get

$$R_{\bar{n}} = \frac{N_{\bar{p}}}{\tau} \cdot \frac{\sigma_{CEX}}{\sigma} \qquad \sigma_{CEX} = \text{charge exchange cross-section} \qquad (6)$$

The optimal antineutron flux is obtained when the stored beam lifetime is only determined by the antiproton interaction in the target and when $N_{\bar{p}}/\tau$ is equal to the antiproton accumulation rate (10^6 s^{-1}). The antineutron rate can only be maximized by optimizing σ_{CEX}/σ. While at high energies $\sigma_{CEX}/\sigma \approx \sigma_{CEX}/\sigma_{st} \approx 0.06$, the antineutron rate at low energies depends strongly on the ratio $\sigma_{CEX}/\Delta\sigma$.

Between 300 MeV/c and 900 MeV/c it is well fitted[2] by

$$\sigma_{CEX} = 17.34 \frac{\sqrt{1 - \left(\frac{0.098}{p_{\bar{p}}}\right)^2}}{1 + 2.0p_{\bar{p}}^2 - 0.45p_{\bar{p}}} \qquad p_{\bar{p}} \text{ in GeV/c}$$

This parametrization is used to calculate σ_{CEX}/σ and in turn the total antineutron rate in the low energy region for an acceptance angle of 6 mrad, under the assumption that no other beam losses contribute significantly, i.e. no extraction nor rest gas losses, etc. For these conditions, the total antineutron rate as given by (6) is plotted in Fig.4. This plot shows, for instance, that at 300 MeV/c under a dedicated operation and for an acceptance angle of 6 mrad, more than 1% of the antiprotons can be converted into $\bar{n}$.

Angular distribution of the antineutrons

Experimentally the angular distribution of antineutrons originating from the charge exchange reaction are only known[3,4] at 430 MeV/c, 350 MeV/c and 730 MeV/c. At these energies the differential cross sections show a strong forward production in the CM-system mainly due to pion exchange.

At lower energies it is expected that the production will become isotropical.

In order to get a rough estimate we have evaluated the laboratory angular distribution of the antineutrons under the assumption of an isotropical CM-production for a point-like target and a zero emittance. This is shown in Fig.6 for a few antiproton momenta. At 430 MeV/c we compared the isotropical with the experimentally measured production (Fig.6), and the resulting laboratory distributions.

The effect is that with an isotropical production the small angle forward production is underestimated. We use this assumption, however to derive a conservative estimate for the rate of antineutrons produced into a given forward solid angle. This plotted in Fig.7.

Comparing the isotropical with the experimentally measured production shows, however, that the rates at 430 MeV/c are roughly a factor 3 higher in forward direction.

Multiple scattering blowup versus beam cooling : Equilibrium emittances

The differential equation describing the change of emittance due to multiple scattering beam blowup on the target on the one hand and beam cooling on the other hand is given by :

$$\frac{dE}{dt} = \dot{E}_{ms} + \dot{E}_c$$

where the multiple scattering blowup rate $\dot{E}_{ms}$ on the target is given by [5]

$$\dot{E}_{ms} = 19.2\ \beta_{H,V}\ \frac{\rho d}{\beta^3\gamma^2}\ (\pi \text{ rad m sec}^{-1})$$

$\beta_{H,V}$ = beta values at the target position

β_H = 9.4 m
β_V = 1 m
} from Ref.7

and the cooling rate $\dot{E}_c$ is

$$\dot{E}_c = -\frac{2}{\tau} E$$

τ = amplitude cooling time

The integration of this equation yields

$$\dot{E}(t) = (1 - e^{-\frac{2t}{\tau}})\ \frac{\tau \dot{E}_{ms}}{2} + E_o\ e^{-\frac{2t}{\tau}}$$

E_o = initial beam emittance

The equilibrium beam emittance E_{eq} is practically reached for $t > \tau\ 3/2$

$$\dot{E}_{eq} = \frac{\tau}{2}\,\dot{E}_{ms} = 9.6\tau \cdot \beta_{H,V}\,\frac{\rho d}{\beta^3\gamma^2} \qquad (\pi \text{ rad m})$$

In Fig.8 the required cooling times for an equilibrium horizontal beam emittance of 2.7 π mm mrad (10 mm beam diameter at the target position) and 24 π mm mrad (30 mm beam diameter) are plotted. The conditions are most stringent at lowest energies, where cooling times below 10 seconds are needed. These cooling times can be reached with electron cooling and beam emittances below 2.7 π mm mrad can be achieved for $\bar{p}$-momenta above 250 MeV/c. However, for lower energies the emittance may grow to 30 π mm mrad. In order to obtain a full overlap of the beams, even at lowest energies, and leaving some margin for closed orbit distortions a horizontal cluster beam width of 40 mm is appropriate. This helps also at higher energies where only stochastic cooling is available. If it turns out that shorter cooling times, and in turn, smaller equilibrium emittances can be achieved, the cluster beam width can be reduced correspondingly.

Momentum resolution

The equilibrium momentum spread is essentially given by the balance between intra-beam scattering and momentum cooling and hence depends on the number of stored particles. However, longitudinal cooling is much faster than emittance cooling and equilibrium values below 10^{-3} can be expected. This results in an invariant mass resolution below 0.5 MeV. The momentum spread of antineutrons emerging under small angles are practically defined by the equilibrium antiproton beam momentum spread, while for higher angles the antineutron momentum spectrum is determined by the angular resolution (Fig. 3).

REFERENCE TO THE APPENDIX

1. W. Grein, Nucl.Phys. B131, 255 (1977)

2. R.P. Hamilton et al., Phys.Rev.Lett. 44, 1179 (1980)

3. R. Bizzarri et al., Nuovo Cimento 54A, 456 (1968)

4. M. Bogdanski et al., Phys.Lett. 62B, 117 (1976)

5. W. Hardt, A few simple expressions for checking vacuum requirements in a proton synchrotron, CERN/ISR-300/GS/68-11, (1969)

FIGURE CAPTIONS

Fig.1 Schematic view of an internal cluster beam target for antineutron production

Fig.2 Tentative layout of LEAR ; JET 1, JET 2 possible target position

Fig.3 Antineutron momentum spectrum as function of Θ_{Lab} for antiproton momentum of .10, .12, .15, .2, .6 and 2 GeV/c, Θ_{Lab} is the angle between the antiproton and the antineutron trajectory.

Fig.4 Total production rate of antineutron versus antiproton beam momentum (eq(6), $N\bar{p}/\tau=10^6$)

Fig.5 Antineutron rate (arbitrary scale) as a function of cos Θ_{Lab} for antiproton momenta of 120, 150 200, 300 and 400 MeV/c assuming isotropical production in the CM system.

Fig.6 a) same as Fig.5 for 430 MeV/c
b) same as Fig.6a using measured[3] $d\sigma/d\Omega$

Fig.7 Number of antineutrons produced into forward angle of 14mstrd and 1.7 mstrd respectively assuming isotropical CM production and arrow indicates the increase of the antineutron rate, if a CM production according Ref.3 is used at 430 MeV/c.

Fig.8 Required cooling times to obtain a horizontal equilibrium beam emittance of 24 π mm mrad and 2.7 π mm mrad respectively when operating a 2.10^{-10} q/cm^2 thick internal target.

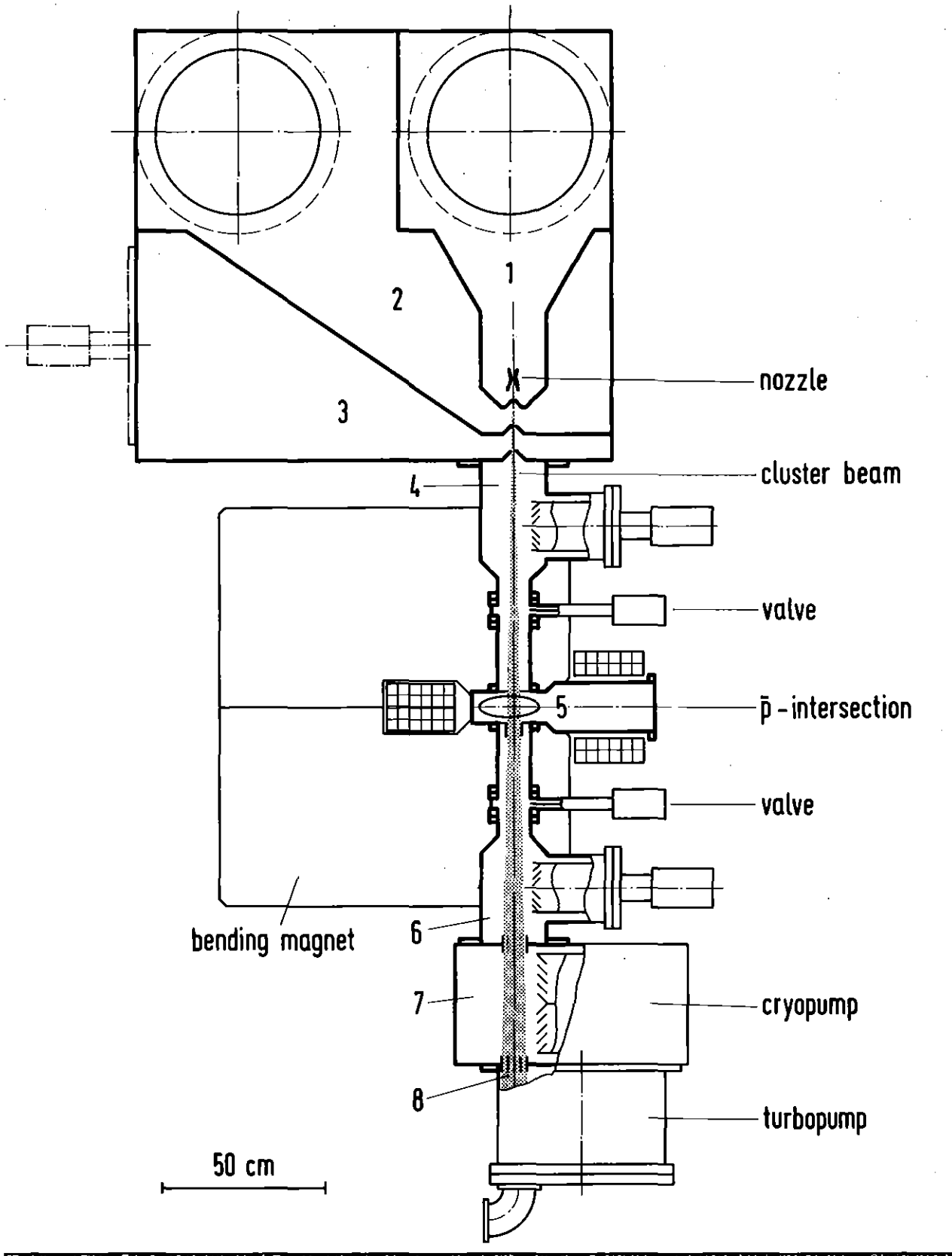
1
2
3
nozzle
cluster beam
4
valve
5
p̄ - intersection
valve
bending magnet
6
7
cryopump
8
turbopump
50 cm

Fig.1

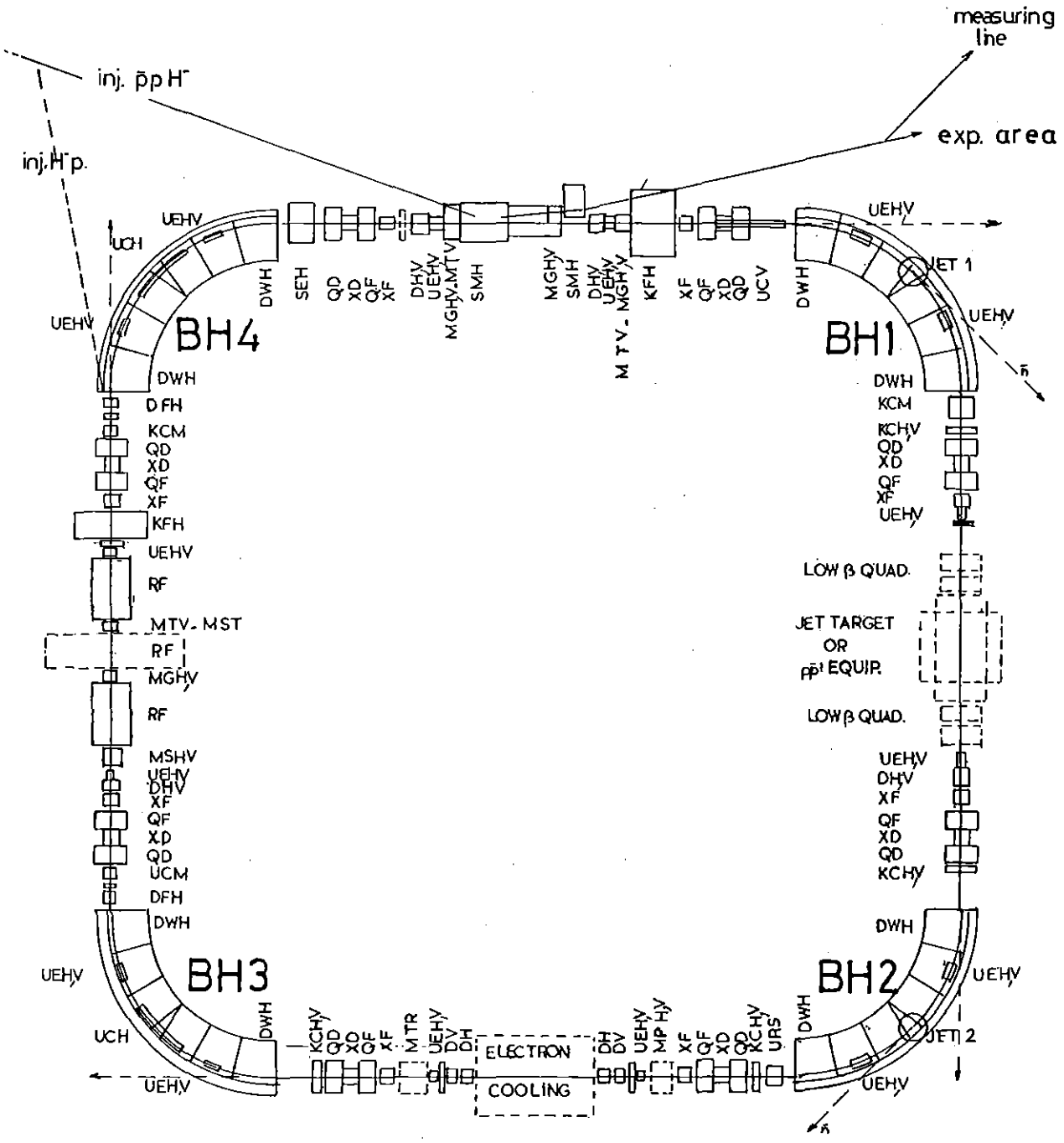
measuring line
inj. p̄p H⁻
exp. area
inj. H⁻p.
BH4
BH1
BH3
BH2
UEHV
UCH
DWH
SEH
QD
XD
QF
XF
DHV
UEHV
MGHV.MTV
SMH
MGHV
SMH
DHV
UEHV
MTV-MGHV
KFH
XF
QF
XD
QD
UCV
JET 1
DFH
KCM
QD
XD
QF
XF
KFH
RF
MTV-MST
MGHV
MSHV
UCM
LOW β QUAD.
JET TARGET
OR
p̄p EQUIP.
KCHV
URS
MTR
DV
DH
ELECTRON
COOLING
MPHV
JET 2

Fig.2

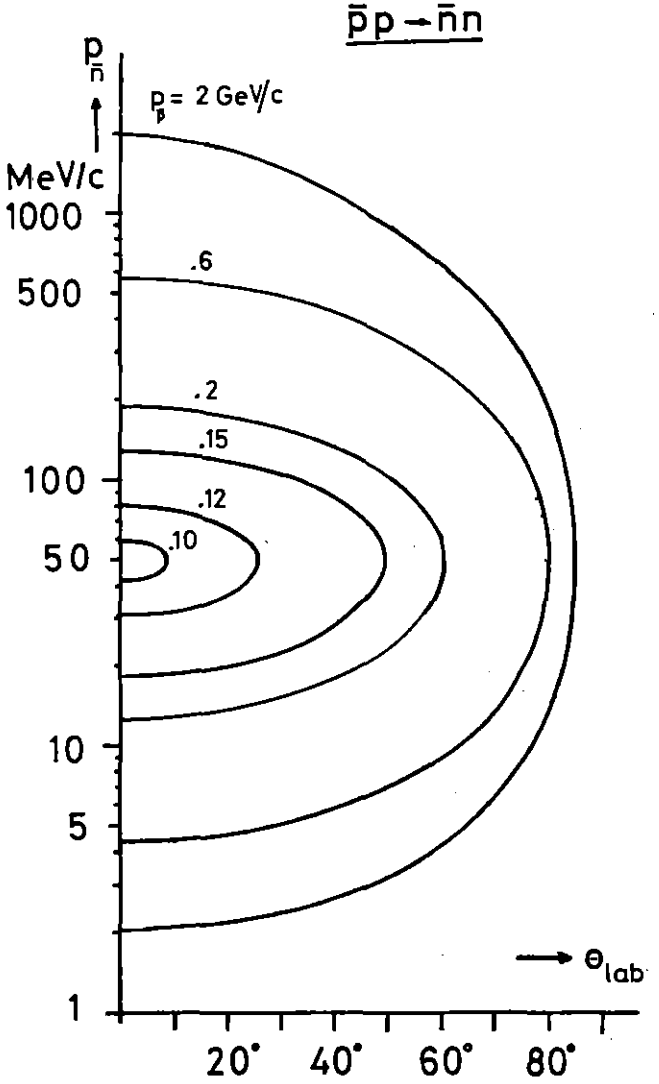
$\bar{p}p \to \bar{n}n$
$p_{\bar{n}}$
MeV/c
$p_{\bar{p}}$ = 2 GeV/c
1000
500
100
50
10
5
1
.6
.2
.15
.12
.10
θ_{lab}
20°
40°
60°
80°

Fig. 3

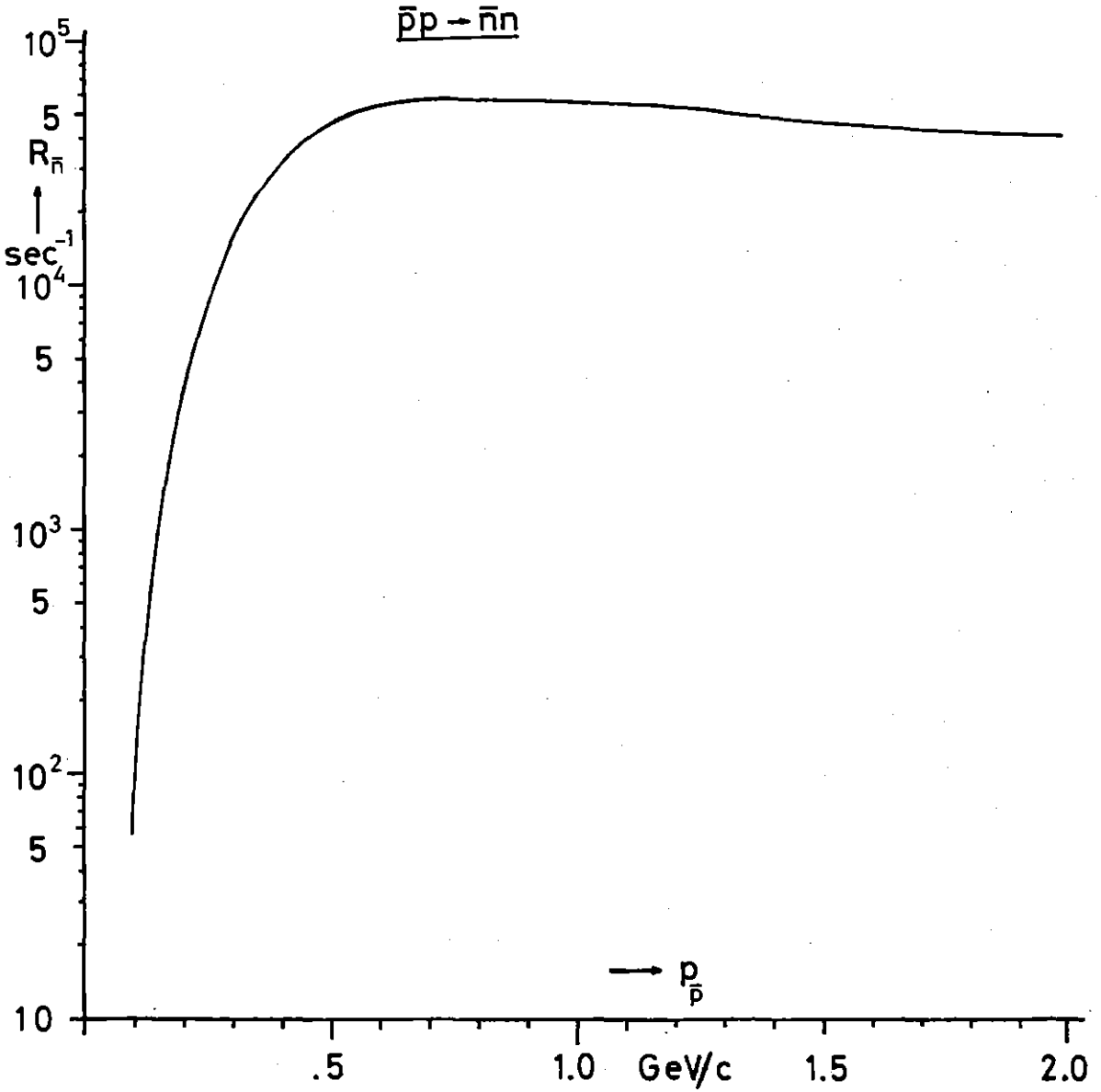
$\bar{p}p \to \bar{n}n$
10^5
5
$R_{\bar{n}}$
sec^{-1}
10^4
5
10^3
5
10^2
5
10
$p_{\bar{p}}$
.5
1.0
GeV/c
1.5
2.0

Fig. 4

$\bar{p}p \rightarrow \bar{n}n$

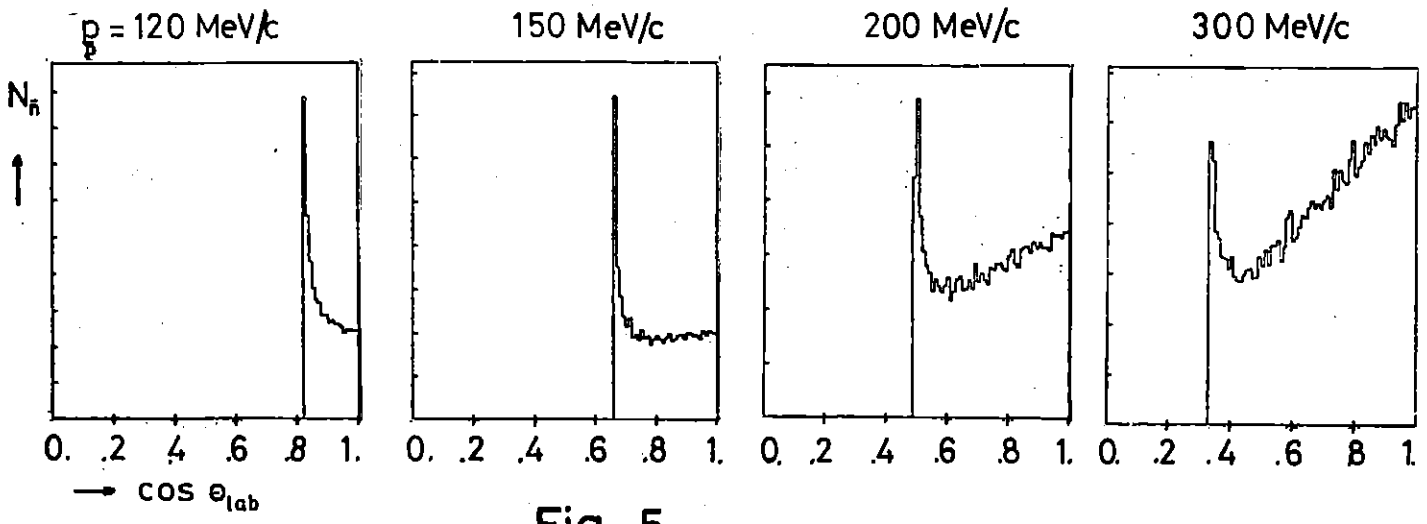

Fig. 5

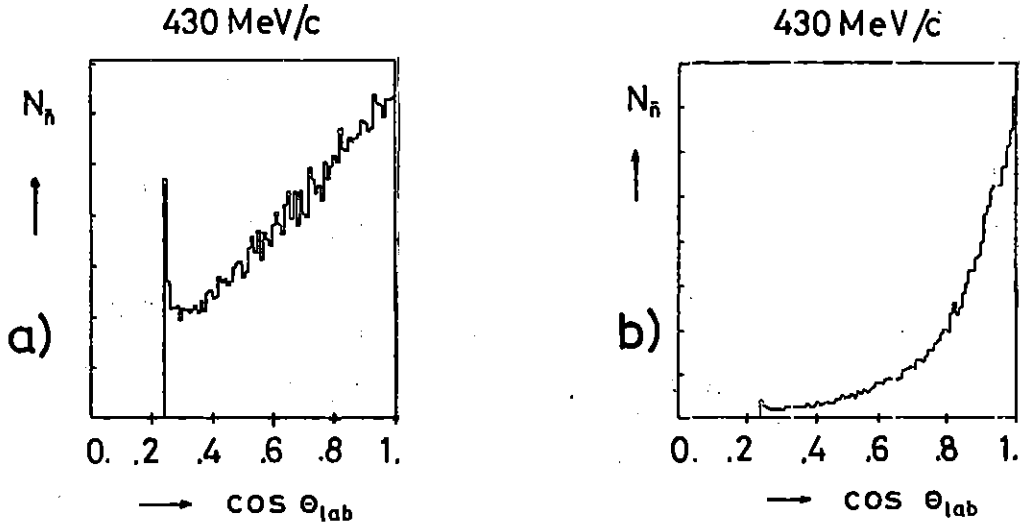

Fig. 6

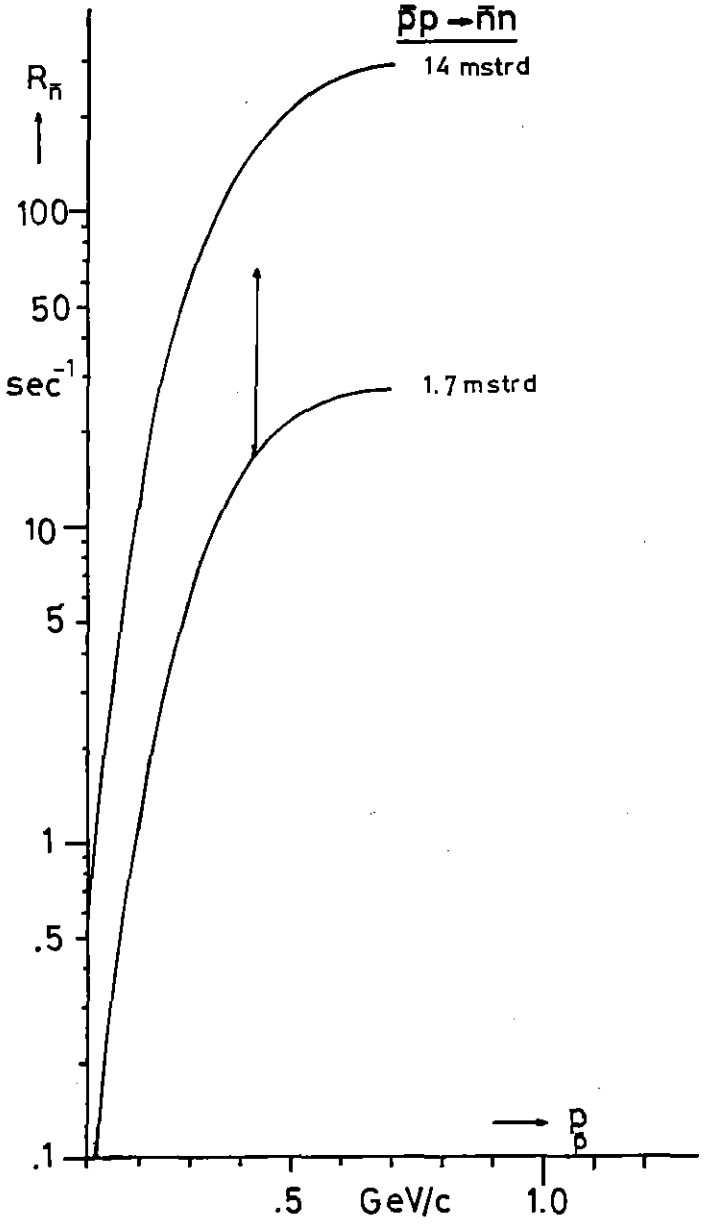
$\bar{p}p \to \bar{n}n$
14 mstrd
1.7 mstrd
$R_{\bar{n}}$
100
50
sec^{-1}
10
5
1
.5
.1
$p_{\bar{p}}$
.5
GeV/c
1.0

Fig. 7

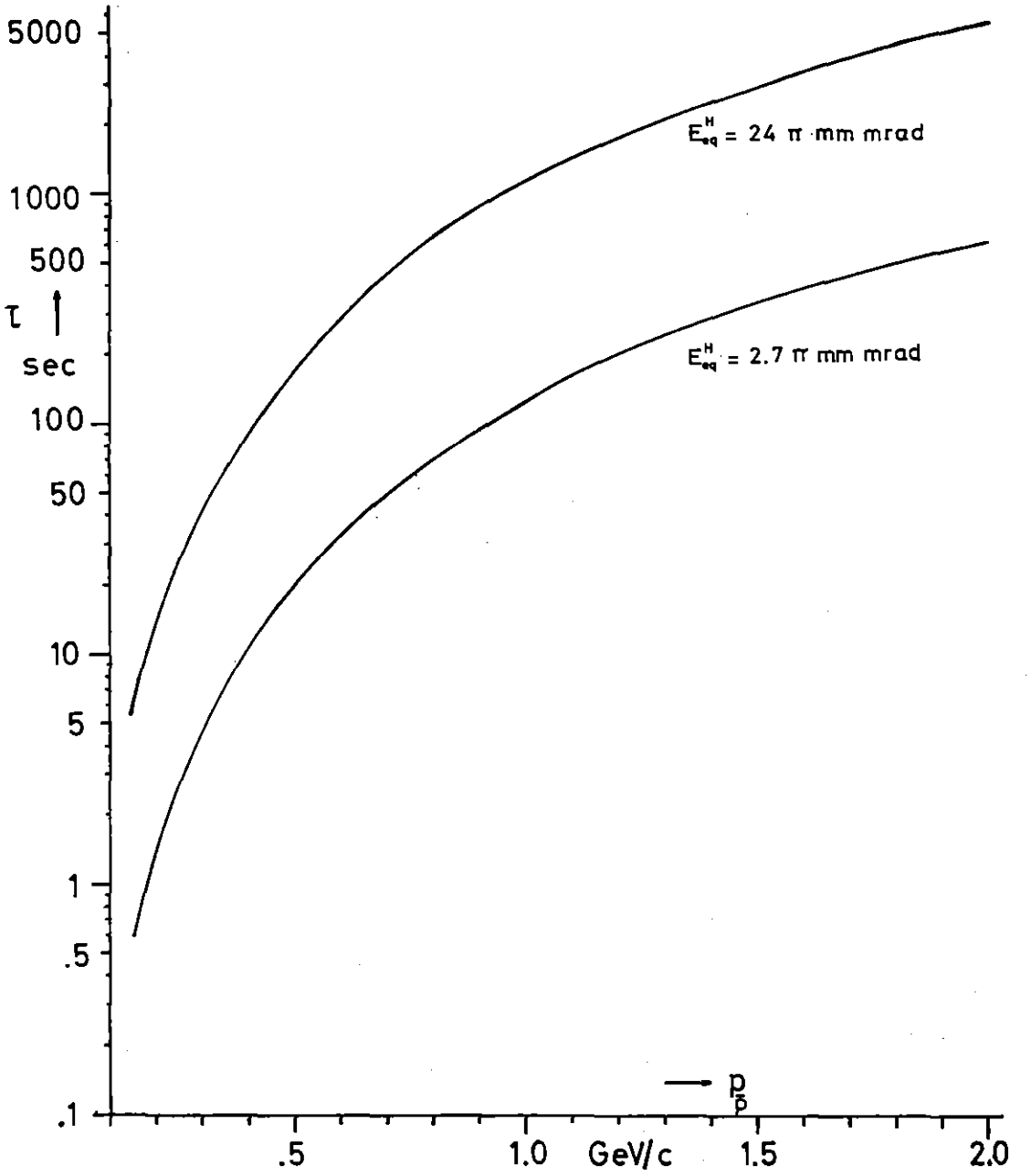
5000
1000
500
τ
sec
100
50
10
5
1
.5
.1
E^H_{eq} = 24 π mm mrad
E^H_{eq} = 2.7 π mm mrad
$p_{\bar{p}}$
.5
1.0
GeV/c
1.5
2.0

Fig. 8